Mecánica Computacional Vol. XXIII, pp. 1911-1929
G.Buscaglia, E.Dari, O.Zamonsky (Eds.)
Bariloche, Argentina, November 2004

SEMI-IMPLICIT SCHEMES FOR FREE SURFACE FLOW SIMULATION

Cassio M. Oishi*, **José A. Cuminato***, **Valdemir G. Ferreira***, **Murilo F. Tomé***, **Antonio Cas Norberto Mangiavacchi†**

*Departamento de Ciências de Computação e Estatística, ICMC,
Universidade de São Paulo, USP
Av. Trabalhador São Carlense, 400, C.P. 668, 13251-900, São Carlos, SP, Brasil
e-mail: *oishi@icmc.usp.br*
jacumina@icmc.usp.br
pvgf@icmc.usp.br
murilo@icmc.usp.br
castelo@icmc.usp.br

†Departamento de Engenharia Mecânica
Universidade do Estado do Rio de Janeiro, UERJ
Rua São Francisco Xavier, 524, 20550-900, Rio de Janeiro, RJ, Brasil
e-mail: *norberto@uerj.br*

Key Words: Incompressible Navier-Stokes equations, Projection methods, Semi-implicit formulation, Numerical simulation, Free surface flows.

Abstract. *This paper present two-dimensional numerical simulation of free surface flows by semi-implicit projection method. The semi-implicit schemes are studied with the purpose of introducing them into the GENSMAC method. The viscous terms are treated by Backward Implicit and Crank-Nicolson methods, and the non-linear convection terms are, explicitly, approximated by the high order upwind VONOS (Variable-Order Non-oscillatory Scheme) scheme. The boundary conditions for the pressure field at the free surface are treated implicitly, and for the velocity field explicitly. The numerical method is then applied to the simulation of free surface and confined flows, and the numerical results show that the present technique eliminates the stability restriction in the original explicit method.*

1 INTRODUCTION AND MATHEMATICAL MODEL

In many fluid flow problems, the viscous forces are dominant, and several numerical techniques have been developed for the solution of this class of flows. In these fluid flow problems, the Reynolds number is often much smaller than 1. Due to this fact, numerical techniques that apply an explicit formulation, as GENSMAC (GENeralized Simplified Marker-And-Cell) method,[1] introduce the parabolic stability restriction, making the time step very small for some applications, justifying the need for methods with better stability properties. In 1947, Crank and Nicolson derived the know famous CN method, an unconditionally stable implicit method to solve the diffusion equation. Approximately ten years later,[2] introduced the Alternating Direction Implicit method (ADI). Many authors (see, for instance,[3,4]) have contributed to the study and understanding of implicit and semi-implicit methods for solving the conservation equations in computational fluid dynamics.

This paper outline a semi-implicit finite difference numerical method for solving incompressible viscous free surface fluid flow problems. By using implicit formulation, this method eliminates the stability restrictions in the explicit formulation. Therefore, it is proposed a modification in the GENSMAC method, adding implicit schemes and treating the boundary conditions for the pressure field at the free surface implicitly. As GENSMAC methodology, the time-marching producere is based on the projection methods ([5] and[6]). It is a finite difference technique based on a staggered grid and solves the full Navier-Stokes equations in primitive variables. In particular, it solves problems with free surfaces.

In non-dimensional conservative form, the mathematical model for incompressible viscous newtonian fluid flows is

$$\frac{\partial \mathbf{u}}{\partial t} + \nabla \cdot (\mathbf{u}\mathbf{u}) = -\nabla p + \frac{1}{Re}\nabla^2 \mathbf{u} + \frac{1}{Fr^2}\mathbf{g}, \tag{1}$$

$$\nabla \cdot \mathbf{u} = 0, \tag{2}$$

where t is time, $\mathbf{u} = [u(x,y,t), v(x,y,t)]$ is the velocity field, $p = p(x,y,t)$ is pressure per unit of mass and $\mathbf{g} = (g_x, g_y)$ is the gravity field. The non-dimensional parameters $Re = LU/\nu$ and $Fr = U/\sqrt{gL}$ are the Reynolds and Froude numbers, respectively, being L and U the length and the velocity scales, and ν is the kinematic viscosity coefficient of the fluid.

2 NUMERICAL FORMULATION

The numerical method proposed to solve the Eqs. (1) and (2) is basically a modification of the GENSMAC method. Firstly, a provisional velocity field $\tilde{\mathbf{u}}$ is calculated from Eq. (1), that is,

$$\frac{\partial \tilde{\mathbf{u}}}{\partial t} = \left\{ -\nabla \cdot (\mathbf{u}\mathbf{u}) - \nabla \tilde{p} + \frac{1}{Re}\nabla^2 \mathbf{u} + \frac{1}{Fr^2}\mathbf{g} \right\}, \tag{3}$$

where $\tilde{p}$ is a provisional pressure. Generally, this provisional velocity field is not a solenoidal one, so $\tilde{p} \neq p$. For $t = t_0$, it is considered that $\mathbf{u}(\mathbf{x}, t_0)$ and $\tilde{\mathbf{u}}(\mathbf{x}, t_0)$ satisfy the same boundary conditions and that on the boundary $\mathbf{u}(\mathbf{x}, t_0) = \tilde{\mathbf{u}}(\mathbf{x}, t_0)$. The main modifications in the

GENSMAC method were the inclusion of the Implicit Formulations (*IF*) for two variations in the projection methods.

The first projection method is based on the solution of the time-discretized Eq. (1), without a provisional pressure gradient (see,[5] referred here as *pressure-free projection method* and denoted by *P1*). Other modification in this equation is the application of implicit methods for the viscous terms. The implicit schemes used in *P1* were the Backward Implicit (*BI*) and Crank-Nicolson (*CN*) methods. In order to improve the temporal accuracy, a 2-step Adams method was employed. This method uses the *CN* approximation for the viscous terms and the explicit Adams-Bashforth for the non-linear convective terms of Eq. (3). This method is known as Adams-Bashforth/Crank-Nicolson (*AB/CN*). Therefore, applying the method *P1* and using the implicit formulations, Eq. (3) is rewritten in the following way

- *P1 - BI method*

$$\tilde{\mathbf{u}} - \frac{\delta t}{Re}\nabla^2\tilde{\mathbf{u}} = \mathbf{u}^n + \delta t\left\{-\nabla\cdot(\mathbf{u}\mathbf{u})^n + \frac{1}{Fr^2}\mathbf{g}^n\right\}. \tag{4}$$

- *P1 - CN method*

$$\tilde{\mathbf{u}} - \frac{\delta t}{2Re}\nabla^2\tilde{\mathbf{u}} = \mathbf{u}^n + \delta t\left\{-\nabla\cdot(\mathbf{u}\mathbf{u})^n + \frac{1}{2Re}\nabla^2\mathbf{u}^n + \frac{1}{Fr^2}\mathbf{g}^n\right\}. \tag{5}$$

- *P1 - AB/CN method*

$$\tilde{\mathbf{u}} - \frac{\delta t}{2Re}\nabla^2\tilde{\mathbf{u}} = \mathbf{u}^n + \delta t\left\{-\frac{3}{2}\nabla\cdot(\mathbf{u}\mathbf{u})^n + \frac{1}{2}\nabla\cdot(\mathbf{u}\mathbf{u})^{n-1} + \frac{1}{2Re}\nabla^2\mathbf{u}^n + \frac{1}{Fr^2}\mathbf{g}^n\right\}. \tag{6}$$

Using the theory of the projection methods, a general velocity field can be decomposed into a tentative $\tilde{\mathbf{u}}$ and the gradient of a potential $\nabla\psi$. In the *P1* method, the function ψ is calculated in the whole domain.

The second projection method used in this work is based on the method with the provisional pressure gradient as in Eq. (3) (see,[6] referred to *incremental-pressure projection methods* and denoted here by *P2*). In the same manner as in the method of *P1*, the viscous terms were taken implicitly. Equation (3) for *P2* becomes

- *P2 - BI method*

$$\tilde{\mathbf{u}} - \frac{\delta t}{Re}\nabla^2\tilde{\mathbf{u}} = \mathbf{u}^n + \delta t\left\{-\nabla\cdot(\mathbf{u}\mathbf{u})^n - \nabla\tilde{p} + \frac{1}{Fr^2}\mathbf{g}^n\right\}. \tag{7}$$

- *P2 - CN method*

$$\tilde{\mathbf{u}} - \frac{\delta t}{2Re}\nabla^2\tilde{\mathbf{u}} = \mathbf{u}^n + \delta t\left\{-\nabla\cdot(\mathbf{u}\mathbf{u})^n + \frac{1}{2Re}\nabla^2\mathbf{u}^n - \nabla\tilde{p} + \frac{1}{Fr^2}\mathbf{g}^n\right\}. \tag{8}$$

- *P2 - AB/CN method*

$$\tilde{\mathbf{u}} - \frac{\delta t}{2Re}\nabla^2\tilde{\mathbf{u}} = \mathbf{u}^n + \delta t\left\{-\frac{3}{2}\nabla\cdot(\mathbf{uu})^n + \frac{1}{2}\nabla\cdot(\mathbf{uu})^{n-1} + \frac{1}{2Re}\nabla^2\mathbf{u}^n - \nabla\tilde{p} + \frac{1}{Fr^2}\mathbf{g}^n\right\}. \tag{9}$$

The development of the *P2* method using *IF* is similar to the *P1* method, with the difference that now $\tilde{p} \neq 0$ will be calculated. In the GENSMAC method, the Poisson equation for ψ

$$\nabla^2\psi = \nabla\cdot\tilde{\mathbf{u}}, \tag{10}$$

is applied for the whole domain containing fluid, with the appropriate boundary conditions described in.[1] For the *P1* and *P2* methods using *IF*, besides the Poisson equation, a new equation is imposed on the potential ψ for the fluid free surface. This new equation is calculated from the equation of the pressure at the free surface. At the free surface, it is necessary to impose conditions on the velocity and pressure. These conditions, considering absent surface tension, are summarized as

$$(\mathbf{T}\cdot\mathbf{n})\cdot\mathbf{n} = 0, \tag{11}$$

$$(\mathbf{T}\cdot\mathbf{n})\cdot\mathbf{m} = 0, \tag{12}$$

where $\mathbf{n} = (n_x, n_y)$ is the normal vector, external to the free surface, and $\mathbf{m} = (m_x, m_y)$ is the tangent vector to the free surface. Substituting the total tensor $\mathbf{T} = -p\mathbf{I} + \boldsymbol{\tau}$, where $\boldsymbol{\tau}$ is the stress tensor and $\mathbf{I}$ the identity tensor, in Eqs. (11) and (12) we obtain

$$-p + \frac{2}{Re}\left[\frac{\partial u}{\partial x}n_x^2 + \frac{\partial v}{\partial y}n_y^2 + \left(\frac{\partial u}{\partial y} + \frac{\partial v}{\partial x}\right)n_x n_y\right] = 0, \tag{13}$$

$$2\frac{\partial u}{\partial x}n_x m_x + 2\frac{\partial v}{\partial y}n_y m_y + \left[\frac{\partial u}{\partial y} + \frac{\partial v}{\partial x}\right](n_y m_x + n_x m_y) = 0. \tag{14}$$

The equations for ψ, which is related to p through Eq. (22) for *P1* or Eq. (23) for *P2*, at the free surface are derived from Eq. (13) with all dependent variables discretized implicitly in time, that is, the boundary conditions at the free surfaces are also taken implicitly. The reason for the implicit discretization is that it was observed that: whereas for confined flows (with no free surface), the discretization of just the viscous terms in the time level $n+1$ is enough to make the method stable, it did not happen for problems with free surfaces, where the implicit discretization of the boundary conditions is necessary. The construction of the implicit equations for the variable ψ will be presented below.

Initially, notice that equation (13) discretized implicitly in the time reads

$$-p^{n+1} + \frac{2}{Re}\left[\frac{\partial u^{n+1}}{\partial x}n_x^2 + \frac{\partial v^{n+1}}{\partial y}n_y^2 + \left(\frac{\partial u^{n+1}}{\partial y} + \frac{\partial v^{n+1}}{\partial x}\right)n_x n_y\right] = 0. \tag{15}$$

The implicit equation (15) couples the pressure p and the velocities u and v on the free surface. Hence, the linear system for those unknown cannot be solved independently. This makes the implicit method very expensive. In order to uncouple those system we have to eliminate the velocities u and v from Eq. (15) leaving it solely in term of p(or ψ). In order to do this we shall use the continuity equation (2) and the relationship between p and ψ given by the projection method. We shall be describing below how to achieve this uncoupling. To illustrate the practical use of equation (15) for ψ at the free surface, consider the case where cells on the free surface (SURFACE cells) possess one or more faces in contact with cells with no fluid (EMPTY cells), as illustrated in Fig. 1. More details about the classification of cells in the mesh can be found in.[7]

For the configuration of the Fig. 1, the vector $\mathbf{n} = (1, 0)$ and Eq. (15) can be reduced to

$$p^{n+1} = \frac{2}{Re}\left(\frac{\partial u^{n+1}}{\partial x}\right). \tag{16}$$

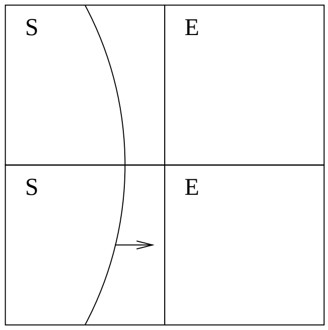

Figure 1: Configuration of a computational cell showing a free surface cells in contact, on its right hand face, with an empty cell.

From the continuity equation Eq. (2) discretized at the time level $n+1$ we get

$$\frac{\partial u^{n+1}}{\partial x} = -\frac{\partial v^{n+1}}{\partial y}, \tag{17}$$

which when substituted into (16) produces

$$p^{n+1} = -\frac{2}{Re}\left(\frac{\partial v^{n+1}}{\partial y}\right). \tag{18}$$

In agreement with the mathematical formulation of the projection methods, the final velocity field can be compute from the equation

$$\mathbf{u} = \tilde{\mathbf{u}} - \nabla\psi, \tag{19}$$

and in this way, the final field velocity in the y direction, is given by

$$v^{n+1} = \tilde{v} - \frac{\partial \psi^{n+1}}{\partial y}. \tag{20}$$

Substituting (20) into (18) yields

$$p^{n+1} = -\frac{2}{Re}\left(\frac{\partial \tilde{v}}{\partial y} - \frac{\partial^2 \psi^{n+1}}{\partial y^2}\right). \tag{21}$$

In agreement with the *P1* formulation, $\tilde{p} = 0$ in the whole domain, therefore the equation for computing the final pressure field in this method is

$$p^{n+1} = \frac{\psi^{n+1}}{\delta t}, \tag{22}$$

while for the method *P2* it is

$$p^{n+1} = \tilde{p} + \frac{\psi^{n+1}}{\delta t}. \tag{23}$$

After substituting (21) into (22) the equation for the potential ψ at the free surface for the method *P1*, is given by

$$\psi^{n+1} - \frac{2\delta t}{Re}\left(\frac{\partial^2 \psi^{n+1}}{\partial y^2}\right) = -\frac{2\delta t}{Re}\left(\frac{\partial \tilde{v}}{\partial y}\right). \tag{24}$$

For the method *P2* substitution of (21) into (23) produces

$$\psi^{n+1} - \frac{2\delta t}{Re}\left(\frac{\partial^2 \psi^{n+1}}{\partial y^2}\right) = -\frac{2\delta t}{Re}\left(\frac{\partial \tilde{v}}{\partial y}\right) - \delta t\tilde{p}, \tag{25}$$

which will be used for the calculation of ψ at the free surface in each case. The construction of the equations for ψ in the other cases where the S cell is in contact with E cells is similar. Notice that Eqs. (24) and (25) together with the Poisson equation (10) give a linear system for ψ, which is uncouple from the other two system for the velocities u and v.

The application of *P1* and *P2* methods for the implicit formulations in GENSMAC result in 3 sparse linear systems: 2 due to the equations that calculate the intermediary velocity and 1 due to the calculation of the potential ψ. When the implicit formulations are applied, for the *BI*, *CN* or *AB/CN* methods, the viscous terms are taken implicitly, and for this it is necessary to solve systems for velocities $\tilde{u}$ and $\tilde{v}$. The linear systems resulting from Eqs. (4)–(9) are sparse, positive defined and symmetric. Due to those properties, an efficient method is the Conjugated Gradient (CG) method. The linear system for ψ is sparse, but non-symmetric, and therefore the method used was the Bi-Conjugated Gradients with Preconditioning (BCGP). Besides the method BCGP other alternatives recommended in the literature for sparse problems exist: the GMRES (Generalized Minimum Residual) and PCGS (Preconditioned Conjugate Gradient Squared) are two examples. More details of the numerical methods using implicit formulations and boundary conditions at the free surfaces can be found in.[7]

2.1 Stability of *P1* and *P2* Methods

The stability restriction imposed for explicit treatment of the viscous terms requires that

$$\delta t_{visc} \leq \frac{Re}{2}\left(\frac{1}{(\delta x)^2}+\frac{1}{(\delta y)^2}\right)^{-1}, \tag{26}$$

where δx and δy are the grid spacing. The application of Implicit Formulations for the viscous terms as in Eqs. (4)–(9), can, in principle, remove the restriction (26). Therefore, the restrictions on δt for *P1* and *P2* using *IF* are more relaxed than in the original GENSMAC code.

2.2 Solution Procedure

The sequence of steps in the solution procedure purports updating the discreet variables, starting from an initial time t_n. The algorithm is described as follow:

- **Step 1**: For the *P1* method, as the pressure gradient $\nabla\tilde{p}$ is eliminated from the formulation and the velocity at the free surfaces is calculate from Eq. (14). For the *P2* method, besides the calculation of the velocity at the free surfaces, the pressure gradient is conserved, $\tilde{p} = p^n$, where p^n is the pressure calculated in the previous time from Eq. (13);

- **Step 2**: Calculate an intermediary velocity field $\tilde{\mathbf{u}}(\mathbf{x}, t)$ in $t = t_n + \delta t$. When the *P1* method is used, Eqs. (4), (5) and (6) can be used. Similarly, when the *P2* method is applied, Eqs. (7), (8) and (9) can be used;

- **Step 3**: Solve the Poisson equation (10) for the potential ψ in the regions that contains fluid, and at the free surface, calculate ψ from new equation derived from Eq. (13). Details of the boundary conditions for the Poisson equation and the equations for ψ at the free surfaces can be found in;[7]

- **Step 4**: Compute the corrected velocity field from Eq. (19);

- **Step 5**: Compute the final pressure field. For the *P1* method, the pressure is computed from Eq.(22) and for the *P2* method, the equation is (23);

- **Step 6**: Update the marker particles positions. The last step in the calculation is moving the marker particles to their new positions. This is performed by solving

$$\frac{\mathrm{dx}}{\mathrm{dt}} = u \qquad \text{and} \qquad \frac{\mathrm{dy}}{\mathrm{dt}} = v, \tag{27}$$

  by Euler's method. The fluid surface is defined by a list containing these particles and the visualization of this boundary is obtained by connecting them by straight lines.

3 DISCRETIZATION OF THE MATHEMATICAL MODEL

Equations (1) and (2) are approximated in a staggered mesh. In this mesh, the pressure is stored at cell centers and the components of the velocity u and v are stored in the middle of the lateral faces. As in,[1] the viscous terms and the pressure gradient in Eqs. (4)–(9) are approximated by central differences, whereas the time derivatives are approximated by forward differences (Euler explicit). The convective terms are discretized by the VONOS scheme (see[8]), which is a bounded upwind technique. For solving the conservation equations, the Freeflow2D (see[9]) simulation environment was used. This systems is composed of three module: a modeling module (modeler) a simulation module (simulator, which implements the full Navier-Stokes equations and mass conservation equation) and the visualization module (visualizator).

4 NUMERICAL EXPERIMENTS

In this section, numerical results using the implicit formulations are presented. The main aim in the comparison is assessing the efficiency of *P1* and *P2* methods using *BI*, *CN* and *AB/CN* formulations, in relation the explicit method for problems with $Re < 1$. In relation to the explicit method, the results are encouraging, in terms of accuracy and efficiency. The following test cases are considered.

4.1 *Hagen-Poiseuille* flow

The validation of the numerical results using *P1* and *P2* methods with *IF* was performed on the flow of a fluid between two parallel plates. In this test case, comparisons between the numerical solutions and analytical solution are feasible (seen[10]). In this simulation, it is considered two parallel plates separated by a distance $L = 1$, forming a channel, that in the beginning is empty and the fluid is injected in the entrance region of the channel with parabolic velocity profile. The *P1* and *P2* methods using *IF* were applied using three meshes, defined respectively as coarse (**M1**, where $\delta x = \delta y = 0.1$m); middle (**M2**, where $\delta x = \delta y = 0.05$m), and fine (**M3**, where $\delta x = \delta y = 0.025$m) meshes. It can be observed from Fig. (2) that the numerical results are similar to the analytical solution, that is, the numerical values obtained by the *P1* and *P2* methods using *IF*, on the three meshes, are in good agreement with the analytical solution. In order to show the convergence of the methods presented in this work the relative error (*Er*), in the l_2 norm, between the numerical solutions and the analytical was calculated. These results are presented in Tab. (1). In table (2) is presented the CPU time for the time $t = 20s$ in the mesh **M2**. For creep flow problems, the *IF* was more stable than the original explicit method. Table (3) shows the δt allowed by implicit and explicit formulations. The methods that use the formulation *BI* admitted values of δt larger than the other formulations. When the Re decreases, the restriction on the time step for the explicit method Eq. (26) was overcome by the *P1* and *P2* methods using *IF*. From Tab. (3), it can be seen that the methods using the formulation *BI* demanded a δt about 500 the 500000 larger times than the explicit method, when Re decreases, while the formulations *CN* and *AB/CN* presented δt about 20 times bigger, independent of Re.

Table 1: Results of δt and error (*Er*) for *Hagen-Poiseuille* flow for $Re = 0.1$ in the meshes **M1**, **M2** and **M3**.

Method	**M1**		**M2**		**M3**	
	δt(s)	*Er*	δt(s)	*Er*	δt(s)	*Er*
Explicit	1.0×10^{-4}	2.5E−05	2.5×10^{-5}	1.8E−06	6.25×10^{-6}	1.3E−07
P1-BI	1.25×10^{-3}	7.1E−04	2.5×10^{-4}	3.7E−05	6.25×10^{-5}	3.2 E−06
P1-CN	2.0×10^{-3}	5.6E−04	5.0×10^{-4}	4.5E−05	1.25×10^{-4}	3.2E−06
P1-AB/CN	2.0×10^{-3}	1.6E−04	5.0×10^{-4}	2.5E−05	1.25×10^{-4}	2.1E−06
P2-BI	1.0×10^{-2}	2.5E−05	1.25×10^{-2}	1.8E−06	6.25×10^{-3}	1.2E−07
P2-CN	2.0×10^{-3}	2.5E−05	5.0×10^{-4}	1.8E−06	5.0×10^{-4}	1.1E−07
P2-AB/CN	2.0×10^{-3}	2.5E−05	5.0×10^{-4}	1.8E−06	5.0×10^{-4}	1.1E−07

Table 2: Results of error (*Er*), δt and CPU time for *Hagen-Poiseuille* flow for $Re = 0.1$ in the mesh **M2**.

Method	*Er*	δt(s)	**CPU time**-(m:s)
Explicit	1.8691×10^{-6}	2.5×10^{-5}	$104 : 40$
P1-BI	3.6879×10^{-5}	2.5×10^{-4}	$25 : 08$
P1-CN	4.5363×10^{-5}	5.0×10^{-4}	$22 : 41$
P1-AB/CN	4.5363×10^{-5}	5.0×10^{-4}	$30 : 41$
P2-BI	1.8689×10^{-6}	1.25×10^{-2}	$5 : 20$
P2-CN	1.8691×10^{-6}	5.0×10^{-4}	$24 : 01$
P2-AB/CN	1.8691×10^{-6}	5.0×10^{-4}	$25 : 29$

Table 3: Limit of stability for δt(s) in *Hagen-Poiseuille* flow over the mesh **M2**, with values different for Re.

Method	$Re = 0.1$	$Re = 0.01$	$Re = 0.001$	$Re = 0.0001$
Explicit	2.5×10^{-5}	2.5×10^{-6}	2.5×10^{-7}	2.5×10^{-8}
P1-BI	1.25×10^{-2}	1.25×10^{-2}	1.25×10^{-2}	1.25×10^{-2}
P1-CN	5.0×10^{-4}	5.0×10^{-5}	5.0×10^{-6}	5.0×10^{-7}
P1-AB/CN	5.0×10^{-4}	5.0×10^{-5}	5.0×10^{-6}	5.0×10^{-7}
P2-BI	1.25×10^{-2}	1.25×10^{-2}	1.25×10^{-2}	1.25×10^{-2}
P2-CN	5.0×10^{-4}	5.0×10^{-5}	5.0×10^{-6}	5.0×10^{-7}
P2-AB/CN	5.0×10^{-4}	5.0×10^{-5}	5.0×10^{-6}	5.0×10^{-7}

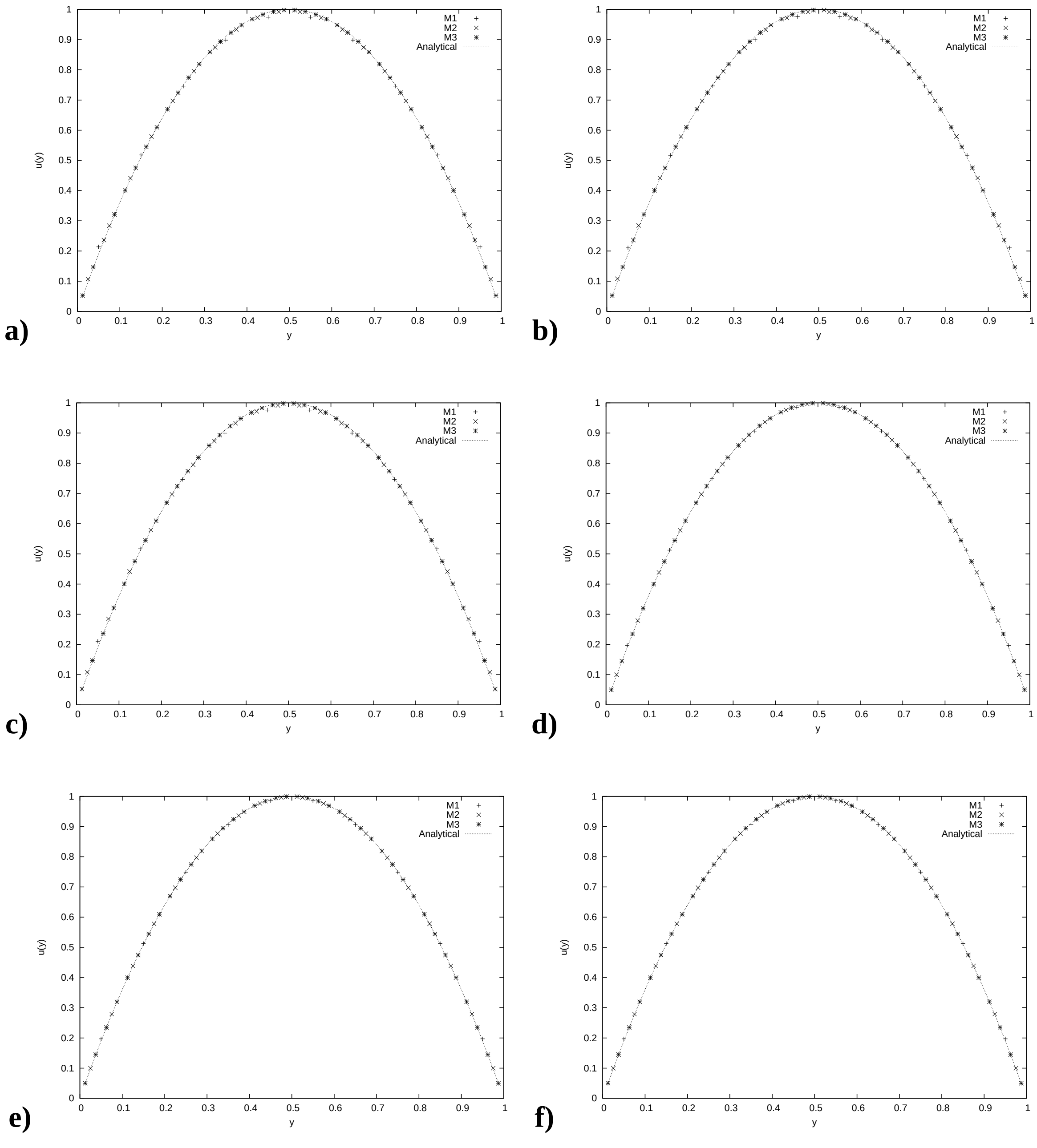

Figure 2: Comparison between numerical solutions obtained by *P1* and *P2* methods using *IF* and analytical solution, over three grids and $Re = 0.1$. **a)-c)** *P1* method using the formulations *BI*, *CN* and *AB/CN*, and **d)-f)** *P2* method using the formulations *BI*, *CN* and *AB/CN*, respectively.

4.2 Impinging Jet

In spite of the purpose of this work to be solving free surface flow at low Reynolds number applying implicit techniques, tests were also accomplished in problems at high Reynolds number showing the efficiency of those methods for problems at moderate Reynolds number. The implicit schemes introduced in the previous section were employed to simulate the flow of an impinging jet onto an impermeable rigid surface, under gravity. For this problem, the Reynolds number, based on the inlet velocity $U = 1.0$m/s and nozzle diameter $L = 0.010$m, is $Re = 5 \times 10^3$, and the Froude number is $Fr = 3.19254$. The grid used was 800×40 cells ($\delta_x = \delta_y = 0.00050$m).

Figures 3 and 4 show a comparison between the numerical solution and the exact solution derived by.[11] This picture shows the non-dimensional free surface of the fluid $(h/0.5L)$ plotted against the non-dimensional distance $(x/0.5L)Re^{-1}$. The numerical results were produced by the implicit numerical schemes and plotted at time $t = 4.0s$. One can see from this picture that there is a good agreement between the numerical solution and Watson's exact solution. It is also worth noting that, for convergence study, this problem was solved by using two other coarser meshes. It is also noticed that for this problem, the numerical results obtained by the *P1* and *P2* methods are very similar. For flow with $Re = 5000$, the value of δt used by the implicit formulations, it wasn't very superior to that of the explicit method, because the condition of stability Eq. (26), has the number of Reynolds as factor, not restricting the temporary step too much for the explicit method. The value of the δt allowed by the explicit method it was 1.5625×10^{-5}s, while for the methods *P1* and *P2* using *IF*, the restriction of the stability was based on the CFL(Courant-Friedrichs-Lewy) condition, determining $\delta t = 6.0 \times 10^{-5}$s. In this problem, the implicit formulations to *BI*, *CN* and *AB/CN*, allowed the same δt.

4.3 Simulation of Container Filling

In this test case, it is considered the problem of container filling of a newtonian fluid with $Re = 0.1$. In this simulation a comparison of CPU time was made using the *P1* and *P2* methods with *IF*, and the explicit method. For these models, a mesh $\delta_x = \delta_y = 0.00050$m was used for all the methods. The gravitational field acts on the flow and the final time of the simulations was $t = 5$s. An illustration is presented in Fig. (5) where the behavior of the flow can be observed. The results obtained by the *P1* method, using the *BI*, *CN* and *AB/CN* formulations and those by *P2* method using the *BI* and *AB/CN* formulations were very similar to those of the *P2* method using the *CN* formulation.

In Fig. (5) one of the results is presented. The comparison between the methods that use the implicit and explicit formulations, verifying the value of δt allowed for each method, the number of iterations and the CPU time for the time $t = 0.28$s, can be seen in Tab. (4). Again, the implicit formulations overcame the restriction of stability of the original explicit method. These methods used less iterations to obtain the solution at the time $t = 0.28$s.

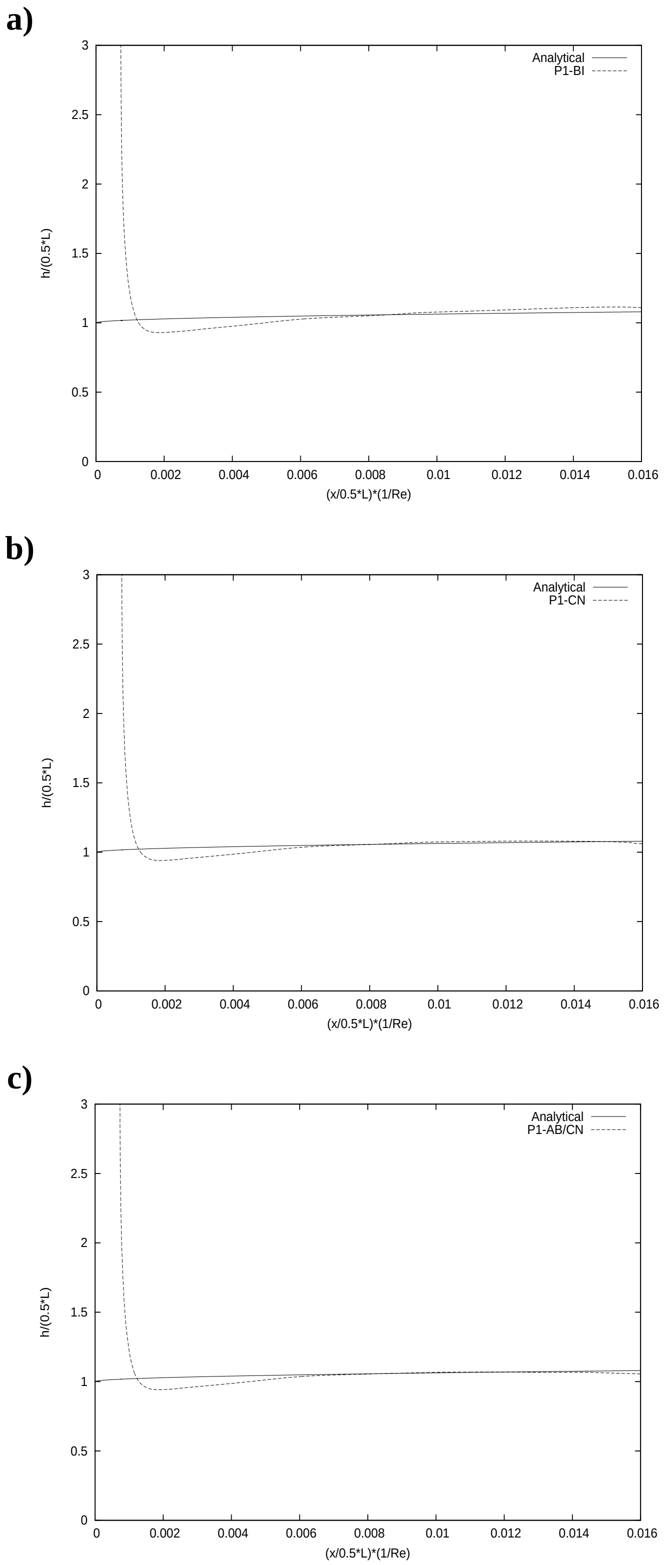

Figure 3: Comparison between Watson's exact solution and the numerical solution for the impinging jet, with $Re = 5 \times 10^3$: **a)-c)** *P1* method using the formulations *BI*, *CN* and *AB/CN*, respectively.

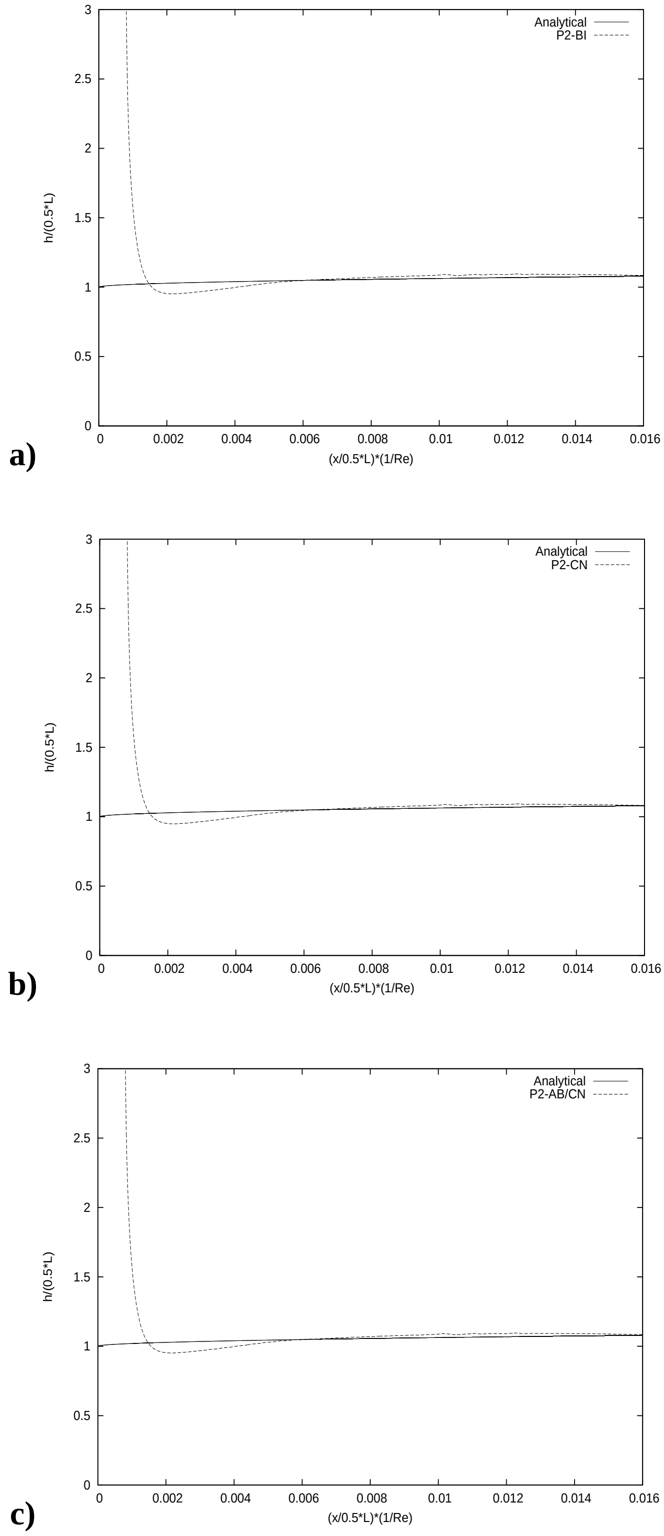

Figure 4: Comparison between Watson's exact solution and the numerical solution for the impinging jet, with $Re = 5 \times 10^3$: **a)-c)** *P2* method using the formulations *BI*, *CN* and *AB/CN*, respectively.

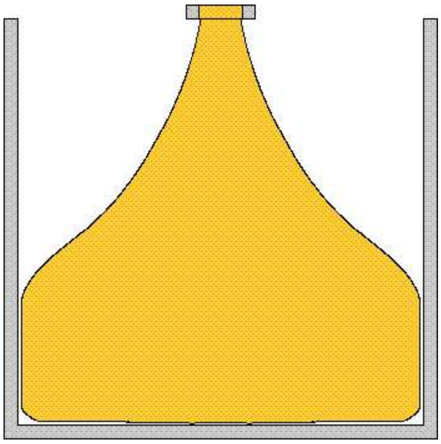

Figure 5: Numerical simulation of container filling, with $Re = 0.1$ and simulation time $t = 0.28$s, for the *P2* method using the *CN* formulation.

Table 4: Results for simulation of container filling. Input data employed: $L = 0.05$m, $U = 1.0$ ms^{-1}, $Re = 0.1$ and $t = 0.28$s.

Method	δt(s)	**Number of iteration**	**CPU time**-(m:s)
Explicit	5.0×10^{-7}	559998	430 : 59
P1-BI	3.0×10^{-5}	11200	41 : 52
P1-CN	1.0×10^{-5}	28000	99 : 16
P1-AB/CN	1.0×10^{-5}	28000	106 : 18
P2-BI	6.0×10^{-5}	8960	21 : 41
P2-CN	1.0×10^{-5}	28000	92 : 51
P2-AB/CN	1.0×10^{-5}	28000	96 : 25

4.4 Comparison with experimental results

Finally, in this test case, qualitative comparisons between numerical results with the experiments described by[12] is assessed. For this model, a mesh of $\delta_x = \delta_y = 0.00050$m was used for all the methods, with the gravitational field acting on the flow and the final time was $t = 5$s. Figure (6) presents the comparison between the numerical solution and an experimental configuration. In this figure, the numerical method used was the *P2* method with the *BI* formulation. The other methods that use the implicit formulations are not displayed because they presented results similar to the *P2* method using the formulation *BI*. The implicit formulations presented, as previously, larger values for δt, overcoming the restriction of the explicit method described by.[12] As an illustration, in Figs. (7) and (8) it is shown comparisons between original explicit method and the *P1* and *P2* methods using *IF*, for the u and v velocities.

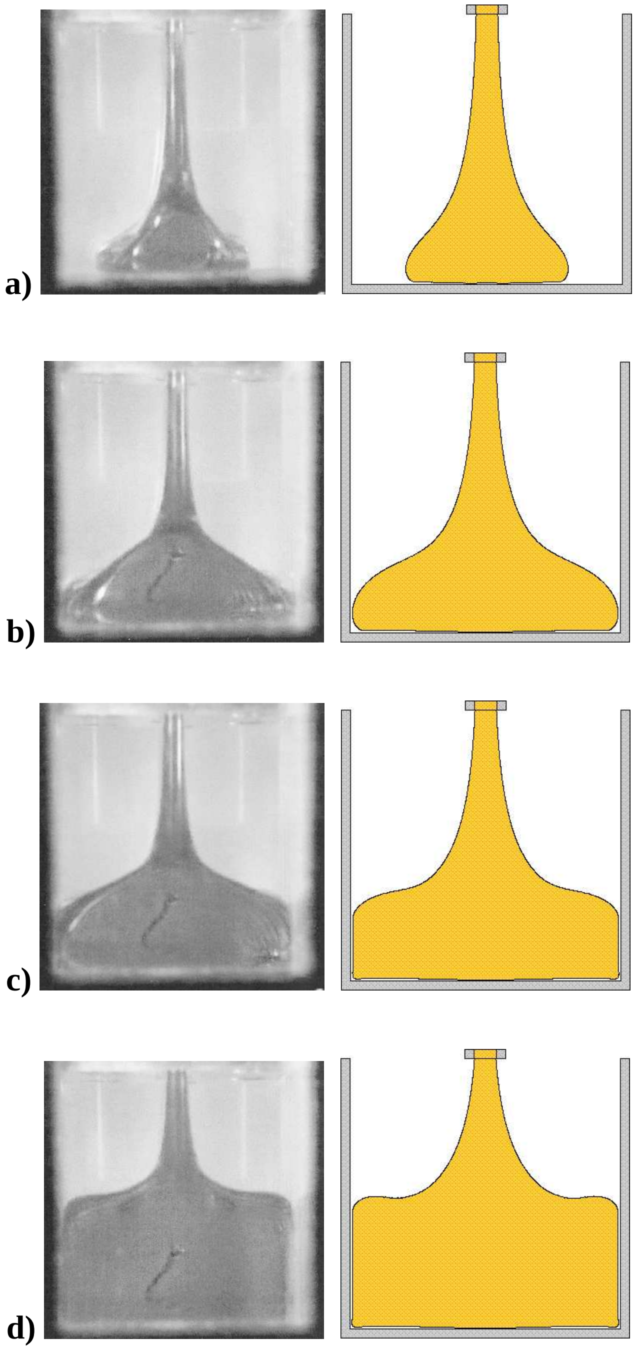

Figure 6: Experimental solution (left) and numerical (right) solution by using *P2* method with the *BI* formulation. **a)**$t = 0.14$s, **b)**$t = 0.22$s, **c)**$t = 0.26$s and **d)**$t = 0.34$s.

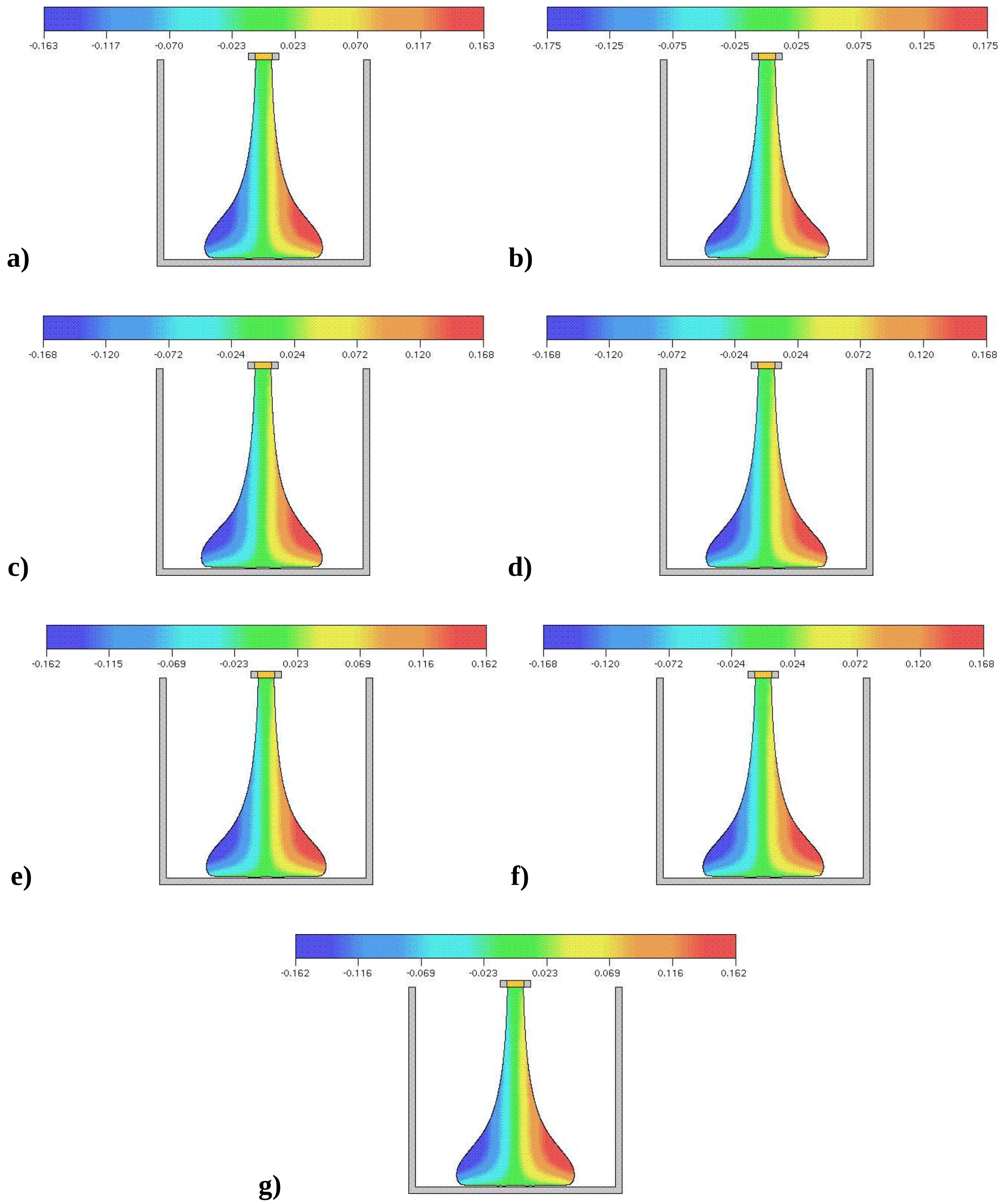

Figure 7: Comparison of velocity field u for $t = 0.14$s. Methods: **a)** Explicit, **b)-d)** *P1* using the *BI*, *CN* and *AB/CN* formulations, respectively, and **e)-g)** *P2* using the *BI*, *CN* e *AB/CN* formulations.

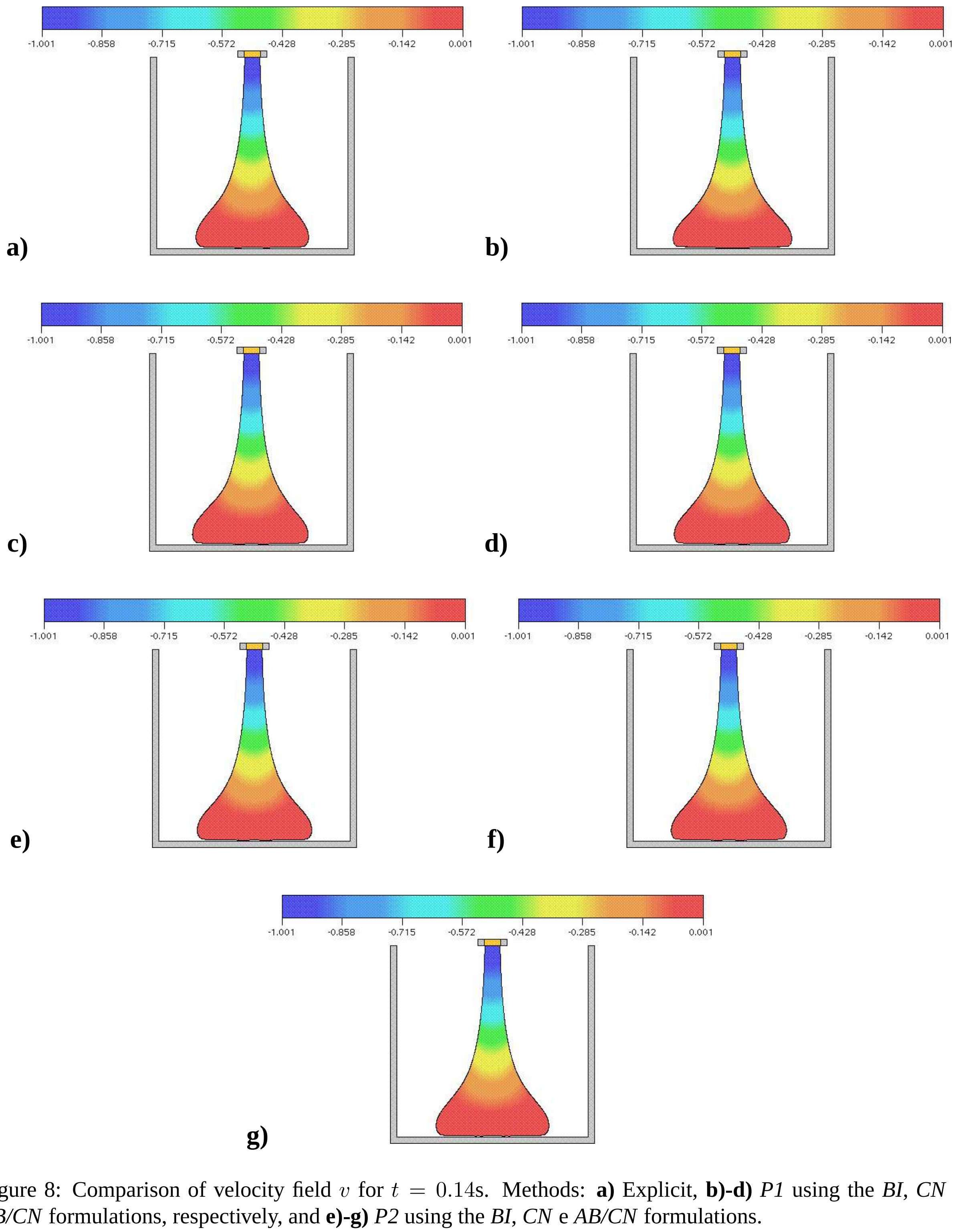

Figure 8: Comparison of velocity field v for $t = 0.14$s. Methods: **a)** Explicit, **b)-d)** *P1* using the *BI*, *CN* and *AB/CN* formulations, respectively, and **e)-g)** *P2* using the *BI*, *CN* e *AB/CN* formulations.

ACKNOWLEDGEMENTS

The authors acknowledge the support of the FAPESP (proc. 00/03385-0 and 01/12540-2) for this work.

5 CONCLUSION

The main purpose of this work is the design and analysis of implicit numerical schemes, which can be used in conjunction with the GENSMAC method for the simulation of transient viscous incompressible newtonian flows. A modification was made to the implicit treatment of boundary conditions for pressure at the free surface. The implicit formulations presented satisfactory results for unsteady free surface flows. The validation showed the comparison between the analytical solution and the numerical solution of the *P1* and *P2* methods using *IF*. The numerical results show the capacity of this semi-implicit methods in simulate fluid flow with free surface. However, the *CN* and *AB/CN* formulations introduced numerical oscillations, and as a consequence, the value of δt allowed was more restricted than that of the *BI* formulation. More details about the numerical oscillations of the method *CN* can be found in[13] and.[3] Although the *CN* and *AB/CN* formulations have allowed a time step larger than that of the original explicit method, the *BI* formulation proved to be stable allowing values of δt very large. Care is recommended in choosing the time step so that numerical accuracy is not affected. In all the simulations, the implicit formulations overcame the value of the time step of the explicit method and, in some cases, the δt was approximately 500000 times larger than the one of the explicit method. The *P1* and *P2* methods using the implicit formulations presented similar errors to those of the explicit method with a very smaller number of iterations. The processing time demanded by the implicit formulations was significantly smaller than those of the explicit formulation. Therefore, the *P1* and *P2* methods using the implicit formulations showed to be capable of solving viscous problems with free surfaces.

REFERENCES

[1] M. F. Tomé and S. McKee. Gensmac: A computational marker-and-cell method for free surface flows in general domains. *Journal of Computational Physics*, **110**, 171–186 (1994).

[2] D.W. Peaceman and H.H. Rachford. The numerical solution of parabolic and elliptic diferential equations. *Journal Soc. Indust. Appl. Math*, **3**, 28–41 (1955).

[3] S. Turek. A comparative study of some time-stepping techniques for the incompressible navier-stokes equations: From fully implicit nonlinear schemes to semi-implicit projection methods. *International Journal for Numerical Methods in Fluids*, **22**, 987–1011 (1996).

[4] W.R. Briley and H. McDonald. An overview and generalization of implicit navier-stokes algorithms and approximate factorization. *Comput. & Fluid*, **30**, 807–828 (2001).

[5] A.J. Chorin. A numerical method for solving incompressible viscous flow problems. *Journal of Computational Physics*, **2**, 12–26 (1967).

[6] P. M. Gresho. On the theory of semi-implicit projection methods for viscous incompress-

ible flow and its implemention via a finite element method that also introduces a nearly consistent mass matrix. *International Journal for Numerical Methods in Fluids*, **11**, 587–620 (1990).

[7] C. M. Oishi. *Análise e implementação de métodos implícitos no sistema FreeFlow2D*. Master's thesis, Universidade de São Paulo, Brasil, (2004).

[8] V.G. Ferreira, M.F. Tomé, A.F. Castelo, J.A. Cuminato, N. Mangiavacchi, and S. McKee. High order upwinding and the hydraulic jump. *International Journal for Numerical Methods in Fluids*, **39**, 549–583 (2002).

[9] A.F. Castelo, M.F. Tomé, M.L. Cesar, J.A. Cuminato, and S. Mckee. Freeflow: An intregated simulation system for three-dimensional free surface flows. *Journal of computers and visualization in science*, **2**, 199–210 (2000).

[10] G. K. Batchelor. *An Introduction to Fluid Dynamics*. Cambridge, (1970).

[11] E. J. Watson. The radial spread of a liquid jet over a horinzontal plane. *Journal of Fluid Mechanics*, **20**, 481–499 (1964).

[12] M.F. Tomé, S. McKee, L. Barratt, D.A. Jarvis, and A.J. Patrick. An experimental and numerical investigations of container filling with viscous liquids. *International Journal for Numerical Methods in Fluids*, **31**, 1333–1353 (1999).

[13] C. Hirsch. *Numerical Computational of Internal and External Flows*, volume 1. A Wiley-Interscience Publication, (1989).